THE PUBLISHING HOUSE
OF THE ROMANIAN ACADEMY

PROCEEDINGS OF THE ROMANIAN ACADEMY, Series A,
Volume 8, Number 2/2007, pp. 000-000

CAVITATION PHENOMENA IN HYDRAULIC VALVES. NUMERICAL MODELLING

Sandor BERNAD*, Romeo SUSAN-RESIGA**, Sebastian MUNTEAN*, Ioan ANTON**

*Center of Advanced Research in Engineering Sciences, Romanian Academy, Timisoara Branch, 300223, Timisoara
**Department of Hydraulic Machinery, "Politehnica" University of Timisoara, 300222 Timisoara, Romania
Corresponding author: Sandor Bernad, E-email: sbernad@mh.mec.upt.ro

The paper presents a numerical simulation and analysis of the flow inside a poppet valve. First, the single phase (liquid) flow is investigated, and an original model is introduced for quantitatively describing the vortex flow. Since an atmospheric outlet pressure produces large negative absolute pressure regions, a two-phase (cavitating) flow analysis is also performed. Both pressure and density distributions inside the cavity are presented, and a comparison with the liquid flow results is performed. It is found that if one defines the cavity radius such that up to this radius the pressure is no larger than the vaporization pressure, then both liquid and cavitating flow models predict the some cavity extent. The current effort is based on the application of the recently developed full cavitation model that utilizes the modified Rayleigh-Plesset equations for bubble dynamics.

Key words: cavitation, vapour volume, vortex cavitation, poppet valve

NOMENCLATURE

h	[m]	poppet displacement	α	[-]	vapour volume fraction
$\dot{m}_v$	[kg/(s.m^3)]	rate of liquid-vapor mass transfer	ρ	[kg/m^3]	density
m_v	[kg/(s.m^3)]	total mass of vapor per liquid-vapor mixture volume	σ	[-]	cavitation number
n	[1/m^3]	number of bubbles per unit volume of liquid	$\vec{u}$	[m/s]	liquid-vapor mixture velocity
$p(r)$	[Pa]	pressure inside de vortex	$\vec{u}_l$	[m/s]	liquid phase velocity
P_0	[Pa]	pressure at the vortex center	$\vec{u}_v$	[m/s]	vapor phase velocity
$\boldsymbol{p_{abs}}$	[Pa]	absolute pressure	α_l	[-]	liquid volume fraction
$\boldsymbol{p_{gauge}}$	[Pa]	gauge pressure	α_v	[-]	vapor volume fractcion
p_{op}	[Pa]	operating pressure	ρ_l	[kg/m^3]	liquid volume fraction density
R	[m]	bubble radius	ρ	[kg/m^3]	liquid-vapor mixture density

1. INTRODUCTION

Cavitation is not nearly as well documented in hydraulic power systems as it is in such water hydraulic systems as pumps, propellers, hydraulic turbines, and hydrofoils. In hydraulic power systems, cavitation most frequently occurs in system valves, pumps, and actuators. Large differences in pressure is a frequent cause of small-scale cavitation in chambers of four-way spool valves, while high frequency motion of a valve-controlled actuator can lead to large-scale cavitation in the cylinder. Another source of cavitation in hydraulic power systems is the improper filling of the pistons on an axial-piston pump. Either during transient loading or under steady-state operation, cavitation can occur in the return chamber of directional control valves because of the large pressure drop across the orifice. It is of interest to know the potential cavitation damage, as well as any effect of cavitation on system performance under both steady and unsteady

flow conditions. Criteria should be established for the onset of cavitation, and damage mechanisms need be identified once cavitation is extensive.

In many engineering applications, cavitation has been the subject of extensive theoretical and experimental research since it has predominantly been perceived as an undesirable phenomenon. This is mainly due to the detrimental effects of cavitation such as erosion, noise and vibrations, caused by the growth and collapse of vapour bubbles.

The flow inside the poppet valve is a complex process which is strongly dependent on the details of the valve geometry, the fluid properties and the operating conditions. Separation and re-attachment of jets can have a profound effect on the flow pressure and force characteristics as well as influencing the susceptibility to cavitations.

Hydraulic valves differ from process control valves in application and design. Hydraulic valves are typically used for controlling pressures and therefore, are of the quick opening type of characteristics. Quick opening valves utilize plugs shaped in the form of a truncated cone with relatively large clearances between the plug and the seat. Or sometimes these valves utilize a disc for a poppet plug. Process control valves on the other hand are used for precise control of the fluid flowrate and are of the linear or equal percentage characteristic. These type valves usually have small clearances between the plug and the seat. Despite these differences, many of the flow phenomena in the hydraulic valve such as recirculation and jet separation and reattachment also occur in the process control valve.

A poppet valve seating-type valve in witch the moving element or poppet, usually spherical or conical shape, moves in a direction perpendicular to its seat. Because of the several advantages that are associated with poppet valves such as ease of manufacture, minimum leakage, and insensibility to clogging by dirt particles, poppet's have been used for as pressure regulators and relief valves. The operation of this type of valve is quite simple. The fluid pressure counterbalances the spring force and allows fluid escape through the annular passage way between the poppet and the seat.

Separating interior flows are of the utmost importance for the performance of wide variety of technical applications [4], [6], [10], [13], [19]. Many industrial designs today have to be compromises between the hydrodynamical function and other competing functions e.g. size or mechanical function. In such compromised designs undesired separation is more likely to occur, this drastically decrease the performance of the design. In such cases, active or passive devices which increase there near wall momentum can be used to remove or reduce the separation [6], [10], [14].

The presence of flow separation in the valve passage and the occurrence of different flow patterns has previously been identified in a number of investigations of different valve geometries. In the extensive work carried out by Tanaka in 1929 [18], it was observed that discontinuities in the flow occurred when investigating the flow quantity across the valve for different valve lifts.

The experimental work of hydraulic valves extends back over many years. Johnston and Edge [11] studied forces on the valve plug as well as the pressure-flow characteristics for several different plug and seat arrangements. Schrenk [22] published work on the pressure-flow characteristics of poppet and disk valves. Stone [20] studied the characteristics of poppet valves with sharp-edged seats, small openings, and low Reynolds number. McCloy and McGuigan [21] studied the effects of the downstream chamber size in a two-dimensional model of a poppet. Some researchers have attempted to analytically predict flow through poppet valves. Von Mises [19] predicted the contraction coefficient for flow through an orifice using potential flow. Fluid forces on the plug are often estimated using simple concepts of fluid momentum change through the valve [10], [20]. Recently CFD has been combined with experimental work to analyze hydraulic valves. Vaughan, Johnston, and Edge [17] modeled the valve reported experimentally by Johnston and Edge [11].

Weclas et al. [23] presented a comprehensive investigation into flow separation in the inlet valve passage using measurement techniques such as discharge coefficient measurements, surface flow visualization using an oil streak technique and detailed flow measurements using LDA. The detailed flow measurements at the valve exit plane and the surface flow visualization showed the flow separation in the valve passage and identified its distribution around the valve periphery for generic inlet port geometries.

A successful design of poppet valves requires a through analysis of both velocity and pressure fields, with the aim of improving the poppet/seat geometry. Technological considerations lead to sharp corners, which in conjunction with very narrow passages produce regions of extremely high gradients in the flow field. As pointed in [2], [7], [15], the poppet flow is not easily suited to classical mathematical analysis.

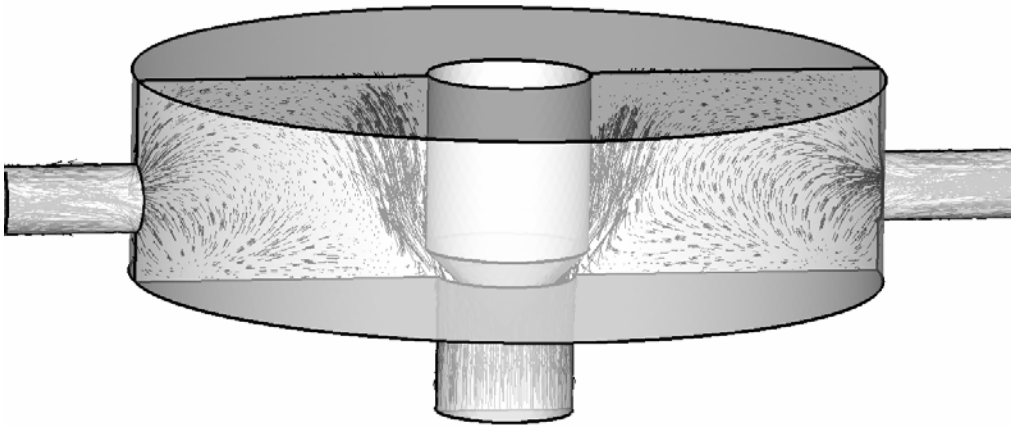

Figure 1. Velocity vector field and streamlines in meridional section plane.

The relative simple geometry, Figure 1, produces a very complicated viscous flow field (Figure 2), which can be realistically investigated only by using Computational Fluid Mechanics. Powerful numerical tools, such as FLUENT software [24], are now available for investigating flows through arbitrary geometries.

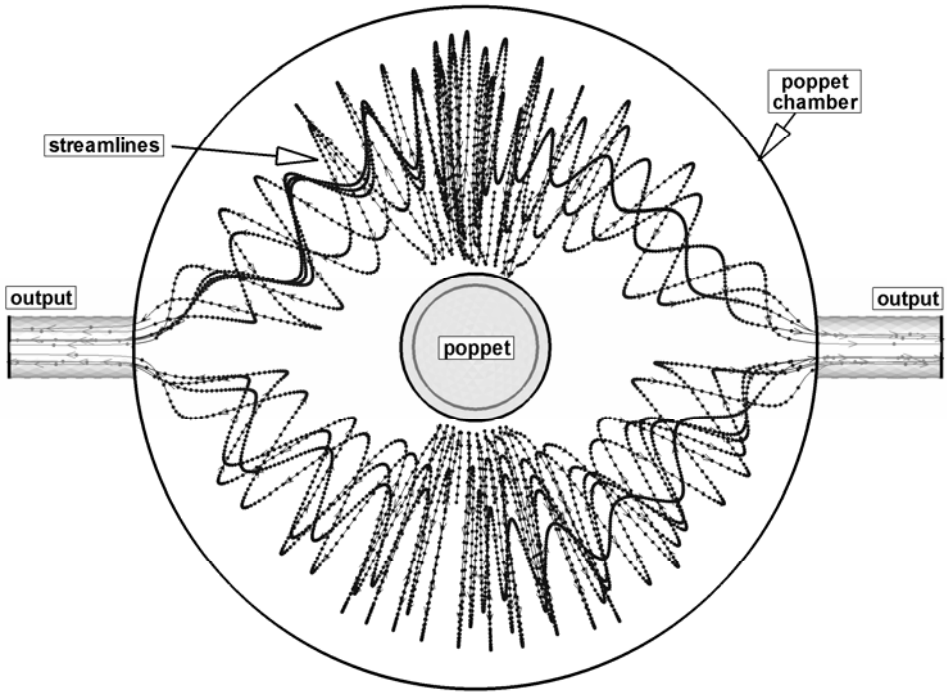

Figure 2. Flow field representation using selected streamlines inside the poppet valve.

Figure 1 show velocity vector field in meridional section plane overlaid with selected streamlines in the 3D computational domain. Velocity vector field in section plane shows the large recirculation region confirming the very strong nature of the helical vortex flow in this poppet valve geometry (Figure 2). The vortex evolution is clearly influenced by the position of the valve outlet section position. Time markers are shown on each streamline, with a unit time step. This representation offers a quick quantitative assessment of the velocity magnitude variation along the streamlines. For example, for the streamline originating near the inlet center, the velocity increases in the valve passage, remains accelerated in the helical vortex region and decreases in the outlet section.

As shown in our previous work [3], the cavitation region is relatively large in a poppet valve chamber, thus we expect a significant change of the flowfield compared with the single phase flow. One of the main goals of this paper is to explore the cavitating flow by using a two-phase flow model. Section 2 presents a simple cavitating flow model employed by the commercial code FLUENT, and results obtained by using this model are presented in Section 5. The main question addressed in this paper is whether or not the single phase flow simulation correctly predicts the vapor cavity radius and location. In addition, we also examine the differences between single-phase and two-phase models in terms of the flow rate and streamline pattern.

2. CAVITATING FLOW MODELING

The FLUENT code employs a generally applicable predictive procedure for turbulent two-phase cavitating flows developed by Cokljat et al. [5]. This model enables formation of vapor from liquid when the pressure drops below the vaporization pressure. If α_v is the vapor volume fraction, then the continuity equation for the vapor phase is,

$$\frac{\partial}{\partial t}\left(\alpha_v \rho_v\right) + \nabla \cdot \left(\alpha_v \rho_v \vec{u}_v\right) = \dot{m}_v , \tag{1}$$

where $\vec{u}_v$ is the velocity of the vapor phase, ρ_v is the vapor density, and $\dot{m}_v$ is the rate of liquid-vapor mass transfer. Obviously, the liquid volume fraction is $\alpha_l = 1 - \alpha_v$ and the mixture density and viscosity are $\rho = (1-\alpha_v)\rho_l + \alpha_v \rho_v$ and $\mu = (1-\alpha_v)\mu_l + \alpha_v \mu_v$, respectively. The continuity equation for the liquid phase,

$$\frac{\partial}{\partial t}\left(\alpha_l \rho_l\right) + \nabla \cdot \left(\alpha_l \rho_l \vec{u}_l\right) = -\dot{m}_v , \tag{2}$$

added to (1) gives the mixture continuity equation,

$$\frac{\partial \rho}{\partial t} + \nabla \cdot \left(\rho \vec{u}\right) = 0 , \tag{3}$$

where the mixture velocity is defined by $\rho\vec{u} = (1-\alpha_v)\rho_l \vec{u}_l + \alpha_v \rho_v \vec{u}_v$. Assuming homogeneous multiphase flow, with no slip between the phases, the same velocity field is shared among the phases, i.e. $\vec{u} = \vec{u}_l = \vec{u}_v$. This assumption is motivated in the cavitation model because no interface between the liquid and vapor phases is assumed, thus allowing the fluids to be interpenetrating. The conservation equation for momentum (with negligible body forces) is:

$$\frac{\partial}{\partial t}\left(\rho \vec{u}\right) + \nabla \cdot \left(\rho \vec{u}\vec{u}\right) = -\nabla p + \nabla \cdot \mu\left[\nabla \vec{u} + \left(\nabla \vec{u}\right)^T\right], \tag{4}$$

Since the cavitation bubble grows is a liquid at low temperature the latent heat of evaporation can be neglected and the system can be considered isothermal. Under these conditions the pressure inside the bubble remains practically constant and the growth of the bubble radius R can be approximated by the simplified Rayleigh equation:

$$\frac{dR}{dt} = \sqrt{\frac{2\left(p_{vap} - p\right)}{3\rho_l}} , \tag{5}$$

where p_{vap} is the pressure of vaporization and ρ_l is the liquid density. The total mass of vapor per mixture volume unit can be written as:

$$m_v = \rho_v \frac{4}{3}\pi R^3 n , \tag{6}$$

with n is the bubble number density. It results,

$$\dot{m}_v = \frac{dm_v}{dt} = \frac{3\rho_v\alpha_v}{R}\frac{dR}{dt} = \frac{3\rho_v\alpha_v}{R}\sqrt{\frac{2(p_{vap}-p)}{3\rho_l}}, \qquad \text{with bubble radius } R = \left(\frac{\alpha_v}{\frac{4}{3}\pi n}\right)^{1/3}, \tag{7}$$

Kubota et al. [12] suggest a minimum of 10^4 and maximum of 10^6 values for the bubble density number n. However, in [2] shows that the bubble initial radius has an insignificant influence on the final radius, as well as on the time for bubble growing up along streamlined bodies. As a result, when a steady cavitating flow configuration is computed, the bubble density number should have little influence on the final result. Our numerical experiments confirm this assertion.

The FLUENT code requires the following methodology for computing cavitating flows. First, a steady solution is obtained for a single phase (liquid) flow, solving (3) and (4). Second, the cavitation model is turned on and the unsteady equations are solved, with the vapor volume fraction, and therefore the liquid-vapor mixture density, as an additional unknown.

Physically, the cavitation process is governed by thermodynamics and kinetics of the phase change process. The liquid-vapor conversion associated with the cavitation process is modeled through two terms, which represents, respectively, condensation and evaporation.

3. THE NUMERICAL APPROACH

To simulate the cavitating flow the numerical code FLUENT [24] was used. The code uses a control-volume-based technique to convert the governing equations in algebraic equations that can be solved numerically. This control volume technique consists of integrating the governing equations at each control volume, yielding discrete equations that conserve each quantity on a control-volume basis. The governing integral equations for the conservation of mass and momentum, and (when appropriate) for energy and other scalars, such as turbulence and chemical species, are solved sequentially. Being the governing equations non-linear (and coupled), several iterations of the solution loop must be performed before a converged solution is obtained. The flow solution procedure is the SIMPLE routine [24]. This solution method is designed for incompressible flows, thus being implicit. The full Navier-Stokes equations are solved. The flow was assumed to be steady, and isothermal. In these calculations turbulence effects were considered using turbulence models, as the k-ε RNG models, with the modification of the turbulent viscosity for multiphase flow. To model the flow close to the wall, standard wall-function approach was used, then the enhanced wall functions approach has been used to model the near-wall region (i.e., laminar sublayer, buffer region, and fully-turbulent outer region). For this model, the used numerical scheme of the flow equations was the segregated implicit solver. For the model discretization, the SIMPLE scheme was employed for pressure-velocity coupling, second-order upwind for the momentum equations, and first-order up-wind for other transport equations (e.g. vapor transport and turbulence modeling equations). Computational domain is discretized using the GAMBIT preprocessor [24]. The flow close to the body surface is of particular importance in the current study, the mesh structure in the computational domain deliberately reflects this concern by heavily clustering the mesh close to the solid surface of the body so that the boundary layer mesh is used encloses the body surface.

4. SINGLE PHASE FLOW SIMULATION AND ANALYSIS

A typical streamline pattern for the liquid flow through the poppet valve is presented in Figure 4. Three main vortices are developed in the poppet valve chamber. The first two vortices, V1 and V2 are rotating counterclockwise and clockwise, respectively, and are generated on the left-hand side and right-hand side,

respectively, of the liquid jet issued from the poppet-seat opening. The third vortex, V3, is generated beyond the valve chamber, in the outflow channel. Such a qualitative analysis of the flow field has been performed also by Dietze [7], who used flow visualization to validate the numerical results, i.e. the streamline pattern. However, Dietze does not provide a quantitative description of the velocity and pressure fields details.

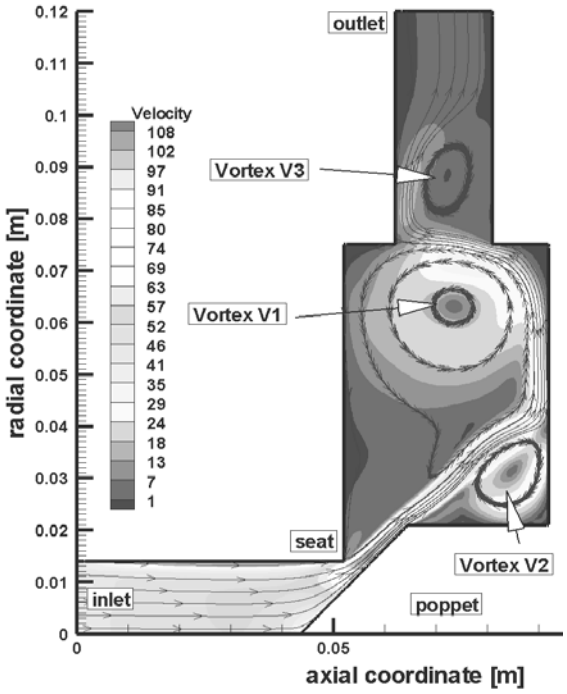

Figure 3. Streamline pattern and pressure field in the meridian half-plane of the poppet valve.

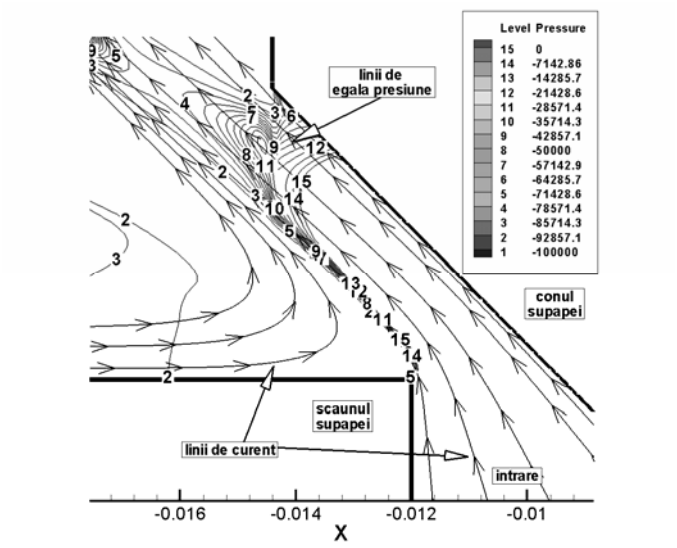

Figure 4. Streamline pattern and pressure field in throttle point vicinity.

The presence of flow separation in the valve passage and the occurrence of different flow patterns has previously been identified in a number of investigations of different valve geometries. In a previous work than authors investigated the flow pattern inside the hydraulic poppet valve chamber for a typical 2D computational domain [2]. In this paper Bernad et al. proposed an original theoretical vortex model thus allowing a parametric study of the poppet valve flow evolution in whole range of poppet displacement. Bulloungh [4] perform the static pressure measurements along the valve cone and seat wall for different

poppet displacement. Visualization of the valve passage flow in a transparent model was investigated for different poppet valve configuration by the Johnston et al [11]. Dietze [7] in his PhD thesis presented a comprehensive investigation into flow separation in the valve passage using measurement techniques and flow visualization to validate the numerical results, i.e. the streamline pattern.

5. CAVITATING FLOW SIMULATION AND ANALYSIS

As mentioned in Section 3, after obtaining a steady single phase (liquid) flow solution, the FLUENT code allows turning on the cavitation model. As a result, vapor formation is enabled where the absolute pressure is smaller than the vaporization pressure. In order to obtain correct results the so-called operating pressure p_{op} must be set to zero (it is set to the atmospheric pressure by default), therefore the gauge pressure p_{gauge} will equals the absolute pressure p_{abs},

$$p_{abs} = p_{op} + p_{gauge}. \tag{10}$$

This is particularly important for obtaining only positive absolute pressure values.

As shown in Figure 5, when the cavitating flow model is used the pressure inside the cavity becomes constant and equals the vaporization pressure, in concordance with cavitation physics. On the other hand, Figure 4 reveals that the pressure exceeds the vaporization pressure at the same radius of approximately 9 mm for both single-phase and two phase models. However, one cannot say that the cavity radius is 9 mm since a continuous transition from vapor to liquid takes place.

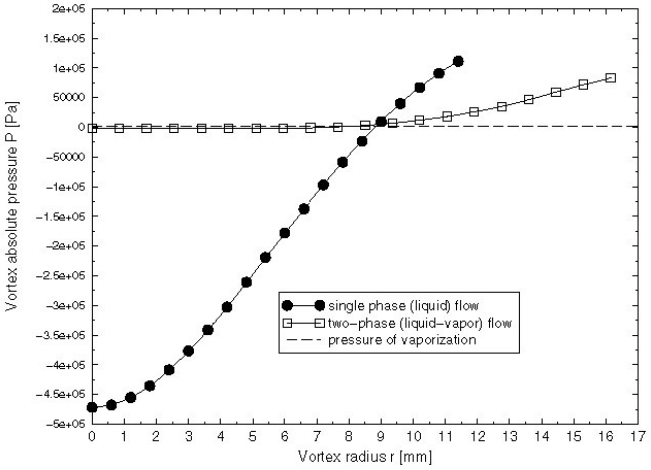

Figure 5. Radial pressure distribution inside the main vortex V1, computed for liquid flow (filled circles, see Figure 3) and liquid-vapor flow (squares).

Figure 6 shows the liquid-vapor mixture density, starting with the vapor region inside the cavity and ending with pure liquid. One can see that there is a large region containing a mixture of liquid and vapor, as it actually happens for industrial cavitation.

A control valve creates a pressure drop in the fluid as it controls the flow rate. The profile of the fluid pressure, as it flows through the valve, is shown in the following graph. The fluid accelerates as it takes a pressure drop through the valve's trim, It reaches its highest velocity just past the throttle point, at a point called the vena contracta. The fluid is at its lowest pressure and highest velocity at the vena contracta. Past the vena contracta the fluid decelerates and some of the pressure drop is recovered as the pressure increases. The pressure in the vena contracta is not of importance until it is lower than the fluid's vapor pressure. Then the fluid will quickly form vapor bubbles and, if the pressure increases above the vapor pressure, the vapor bubbles instantly collapse back to liquid (Figure 6).

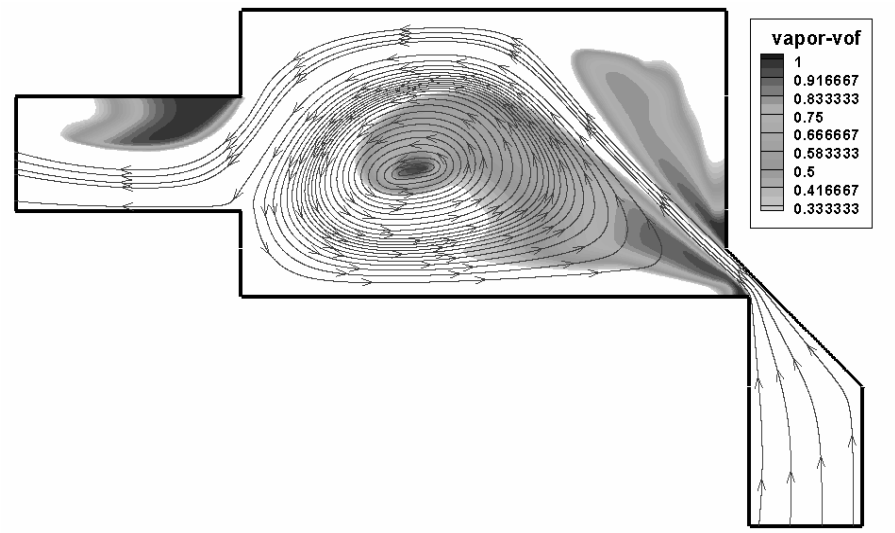

Figure 6. Radial distribution for the liquid-vapor mixture density inside the main vortex (cavity).

The liquid flow rate will increase as the pressure drop increases. However, when cavitation vapor bubbles form in the vena contracta, the vapor bubbles will increasingly restrict the flow of liquid until the flow is fully choked with vapor. This condition is known as "choked flow" or "critical flow". When the flow is fully choked, the flow rate does not increase when the pressure drop is increased.

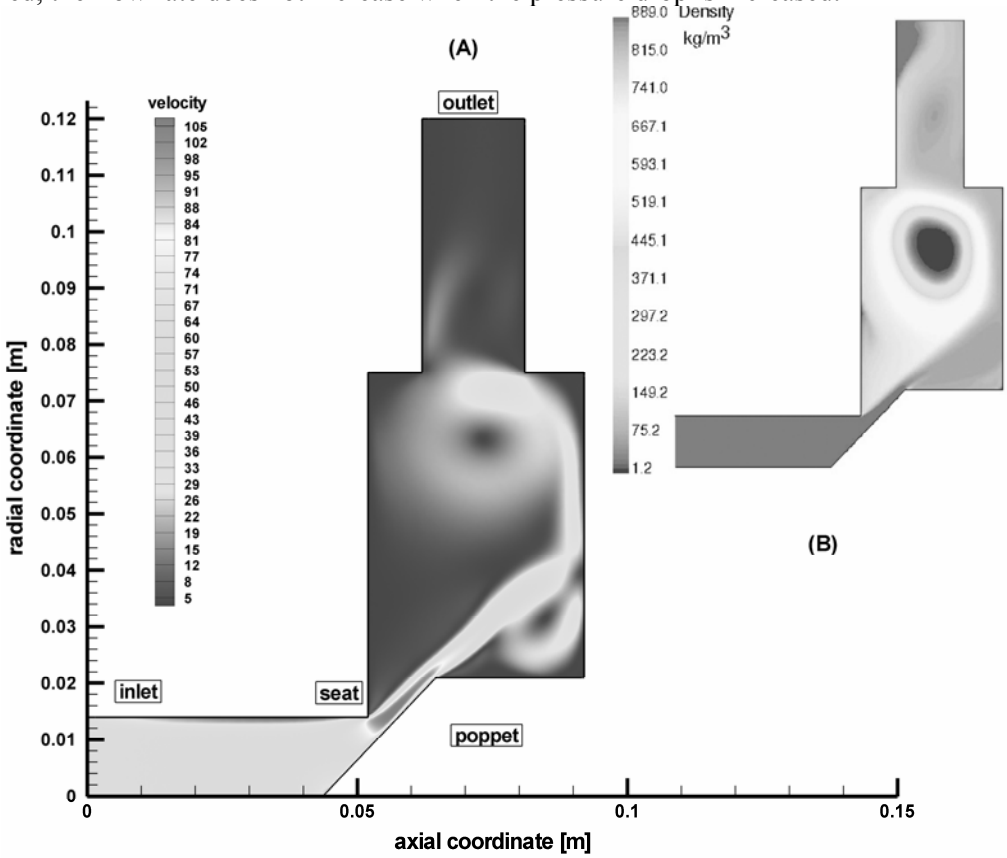

Figure 7. Velocity filed and corespondend liquid-vapour mixture distribution for cavitating flow.

Cavitation will begin at the point of "Incipient Cavitation" and increase in intensity to the point of choked flow. Cavitation at point of "Incipient Cavitation" is not damaging and is almost undetectable. At some point between incipient and choked, the cavitation may damage most trim styles. The location of the "Damage" point varies with trim style and material.

The radial distribution of the density inside the main vortex is presented in Figure 7. One can say that the vapor filled cavity has a radius of 5 mm, but since we have a smooth transition from the vapor region to the liquid region other conventional cavity radii might be defined.

The cavitating flow streamline pattern is not significantly altered in comparison with the one presented in Figure 1. However, one can notice that the main vortex is slightly shifted toward the axis of symmetry and the secondary vortex V2 becomes smaller.

As far as the flow rate is concerned, the liquid flow value is practically the same for cavitating flows. Further investigations are needed to elucidate this issue.

6. CONCLUSIONS

The paper presents a numerical investigation of cavitating flows using the mixture model implemented in the FLUENT commercial code. The inter-phase mass flow rate is modelled with a simplified Rayleigh equation applied to bubbles uniformly distributed in computing cells, resulting in an expression for the interphase mass transfer. This is the source term for the vapor phase transport equation. As a result, the density of the liquid-vapor mixture is allowed to vary from the vapor density up to the liquid density.

The cavitation model is validated for the flow inside the poppet valve chamber. The numerical results agree very well both qualitatively and quantitatively with the experiments. As a result we include that the present cavitational model is able to capture the major dynamics of the cavitating flows inside the hydraulic power equipment.

Cavitation damage problems are more likely to occur with water flow as water has a well-defined vapor pressure and the vapor bubble collapse is instantaneous. Hydrocarbon fluids have a less precise vapor pressure and are often a compound with several vapor pressures [8, 9]. Cavitation damage with hydrocarbon fluids is usually less severe than water, as the bubble collapse is not as sudden and can be cushioned by other vapors. However the vibration and flow noise problems remain [10], [20].

The fluid's inlet pressure is proportional to the amount of energy available to cause cavitation damage. Higher inlet pressures will produce more intense and more damaging cavitation.

The generation and implosion of the vapor bubbles will cause vibration to the valve's poppet that may cause wear between the poppet and the seat.

The generation and implosion of the vapor bubbles will cause significantly elevated flow noise in addition to vibration. The cavitation bubbles will form a vapor plume in the liquid. The larger the plume, the noisier the flow and the more likely it is to cause erosion damage. The size of the plume is dependent on trim style and severity of cavitation.

ACKNOWLEDGMENTS

This work has been supported by Romanian National University Research Council under Grant No. 730/2007. The computation was performed using hardware and software infrastructure on the National Center for Engineering of Systems with Complex Fluids, “Politehnica” University of Timisoara.

REFERENCES

1. BATCHELOR G.K., An Introduction to Fluid Dynamics, Cambridge at the University Press, Cambridge, 1967.
2. BERNAD S., SUSAN-RESIGA R., ANTON I., ANCUŞA V., *Vortex Flow Modeling Inside The Poppet Valve Chamber - Part 2*, Bath Workshop on Power Transmission & Motion Control, PTMC 2001, Bath, UK, 12 – 14 September, 161-176, 2001.
3. BERNAD S., SUSAN-RESIGA R., ANTON I., ANCUŞA V., *Numerical Simulation of Cavitating Flow in Hydraulic Poppet Valve*, In I. Anton, V. Ancuşa, R. Resiga (Eds.), Proceedings of the Workshop on Numerical Simulation for Fluid Mechanics and Magnetic Liquids, Editura Orizonturi Universitare, Timişoara, 140-146, 2001.
4. BULLOUNGH W.A. AND CHIN S.B., *A numerical study of the effects of poppet valve geometry on its flow characteristics*, Proceedings of The Ninth International Symposium on Transport Phenomena in Thermal-Fluids Engineering, Singapore, June 25-28, pp: 579-584, 1996.

5. COKLJAT D., IVANOV V.A., VASQUEZ S.A., *Two-Phase Model for Cavitating Flows*, in Third International Conference on Multiphase Flow, Lyon, France, Available on ICMF98 CD-ROM, paper 224, 1998.
6. DAVIS J.A., STEWART M., *Predicting globe Control Valve performance – part I: CFD modeling*, Journal of Fluid Engineering, Vol. **124**, pp: 772-777, 2002.
7. DIETZE M., *Messung und Berechnung der Innenströmung in hydraulischen Sitzventilen*, Ph.D. Thesis, Düsseldorf, 1996.
8. EIZO URATA, Thrust of poppet valve, Bulletin of JSME, **53**, pp: 1099, 1969.
9. EIZO URATA, *Cavitation Erosion in Various Fluids,* Bath Workshop on Pover Transmission & Motion Control, University of Bath, U.K., 8-10 September, 1999.
10. HENRIK L. SORENSEN, *Numerical and experimental analyses of flow and flow force characteristics for hydraulic seat valves with difference in shape,* Proceedings of the Bath Workshop on Power Transmission & Motion Control, University of Bath, U.K, 1999.
11. JOHNSTON D.N., EDGE K.A., VAUGHAN N.D., *Experimental investigation of flow and force characteristics of hydraulic poppet and disc valves*, Proc Instn.Mech.Engrs. Vol. **205**, pp: 161-171, A01889 ImechE, 1991.
12. KUBOTA A., KATO H., YAMAGUCHI H., *A new modeling of cavitating flows: a numerical study of unsteady cavitation on a hydrofoil section*, Journal of Fluid Mechanics, Vol. **240**, pp.59-96, 1992.
13. MAIER A., SHERLDRAKE T.H., WILCOCH D., *Geometric parameters influencing flow in a axisymmetric IC engine inlet port assembly – part I: valve flow characteristics*, Journal of Fluid Engineering, Vol. **122**, pp: 650-657, 2000.
14. MAIER A., SHERLDRAKE T.H., WILCOCH D., *Geometric parameters influencing flow in a axisymmetric IC engine inlet port assembly – part II: parametric variation of valve geometry*, Journal of Fluid Engineering, Vol. **122**, pp: 658-665, 2000.
15. RESIGA R., BERNAD S.I., ANTON I., *Vortex Flow Modeling Inside the Poppet Valve Chamber*, The Seventh Scandinavian International Conference on Fluid Power, SICFP'01, May 30 - June 1, Linkoping, Sweden, 2001.
16. SAMUEL MARTIN C., Medlarz H., Wiggert D.C., Brennen C., *Cavitation Inception in Spool Valves*, Journal of Fluid Engineering, Vol. **103**, pp: 564-576, 1981.
17. VAUGHAN N.D., JOHNSTON D.N., *Numerical simulation of fluid flow in poppet valves*, Proc Instn. Mech. Engrs., C413/0779 ImechE, pp: 119-127, 1991.
18. TANAKA K., *Airflow Through Suction Valve of Conical Seat*, Aeronautical Research Institute Report, Tokyo Imperial University, Part 1, p. 262; Part 2, p. 361., 1929.
19. VON MISES, R., *The Calculation of Flow Coefficient for Nozzle and Orifice*, VDA, **61**, pp. 21-23, 1916.
20. STONE J. A., *Discharge Coefficients and Steady State Flow Forces for Hydraulic Poppet Valves*, Trans. ASME, **144**., 1960.
21. McCLOY D., and McGUIGAN R. H., *Some Static and Dynamic Characteristics of Poppet Valves*, Proc. Inst. Mech. Eng., **179**, 1964.
22. SCHRENK E., *Disc Valves, Flow Patterns, Resistance, and Loading*, BHRA Publications, T547, 1957.
23. WECLAS M., MELLING A., AND DURST F., *Flow Separation in the Inlet Valve Gap of Piston Engines*, Prog. Energy Combust. Sci., **24**, No. 3, pp.165–195, 1998.
24. FLUENT 6. User's Guide, Fluent Incorporated, 2002.

Received, April 19, 2007